Computers and Chemical Engineering 34 (2010) 146–153

Contents lists available at ScienceDirect

Computers and Chemical Engineering

journal homepage: www.elsevier.com/locate/compchemeng

A simple numerical solution to the Ward–Tordai equation for the adsorption of non-ionic surfactants

Xueliang Li, Ryan Shaw, Geoffrey M. Evans, Paul Stevenson*

Centre for Advanced Particle Processing, University of Newcastle, University Drive, Callaghan, NSW 2308, Australia

ARTICLE INFO

Article history:
Received 21 October 2008
Received in revised form 18 January 2009
Accepted 28 August 2009
Available online 6 September 2009

Keywords:
Diffusion-controlled adsorption
Non-ionic surfactants
Dynamic surface tension

ABSTRACT

A simple numerical scheme for solving the equation of Ward and Tordai (1946) for the diffusion-controlled adsorption of non-ionic surfactants to interfaces is proposed and pseudo-code, as well as C++ source code, is provided. The scheme utilises the trapezium rule of numerical integration and the accuracy and robustness of the method is enhanced by the bisection method of root-finding. The scheme is efficient and flexible in that it can be used with any adsorption isotherm and is readily modified for solving the problem of adsorption onto a convex interface. This scheme is not suggested for the adsorption onto a concave interface and the confusions that have previously arisen in relation to this problem are discussed.

1. The significance of the equation of Ward and Tordai (1946)

The adsorption of a non-ionic surfactant molecule onto an interface is generally considered to be governed by two processes: (1) the diffusion of the surfactant molecule to the sub-surface from the bulk solution; and (2) the adsorption of the molecule from the sub-surface onto the interface. "Diffusion-controlled" models assume a local equilibrium between the sub-surface and the interface. Thus the rate of adsorption is determined by the mass transfer from the bulk solution to the sub-surface, which is described by Fick's law of diffusion. The diffusion equations can be solved by applying numerical methods when proper initial conditions and boundary conditions are provided. An analytical expression is desirable to gain a deeper understanding of the adsorption process. The diffusion equation was first integrated by Ward and Tordai (1946), resulting in an integral equation of the form:

$$\Gamma(t) = 2\sqrt{\frac{D}{\pi}}\left\{c_b\sqrt{t} - \int_0^{\sqrt{t}} c(\tau)\, d(\sqrt{t-\tau})\right\} \tag{1}$$

where t is time since the formation of the fresh surface, D is the coefficient of molecular diffusion and τ is a dummy variable with the units of time. c_b and $c(\tau)$ are the bulk concentration and the sub-surface concentration respectively. The second term within the bracket is the so-called back-diffusion term, and it is similar in form to the convolution integral.

Mysels (1982) applied the superposition method and obtained an analogous equation to the planar Ward–Tordai equation that is applicable to the adsorption onto a convex spherical interface of radius r:

$$\Gamma(t) = 2\sqrt{\frac{D}{\pi}}\left\{c_b\sqrt{t} - \int_0^{t} c(\tau)\, d\sqrt{t-\tau}\right\} + \frac{D}{r}\left\{c_b t - \int_0^{t} c(\tau)\, d(t-\tau)\right\} \tag{2}$$

which can be identically expressed as

$$\Gamma(t) = \sqrt{\frac{D}{\pi}}\left\{2c_b\sqrt{t} - \int_0^{t} \frac{c(\tau)}{\sqrt{t-\tau}}\, d\tau\right\} + \frac{D}{r}\left\{c_b t - \int_0^{t} c(\tau)\, d\tau\right\} \tag{3}$$

This equation was later derived by Lin, McKeigue, and Maldarelli (1990) by means of Laplace transformation and the same routine was repeated by Liu, Wang, and Messow (2005) and Nguyen, Phan, and Evans (2006). Eq. (2) is identical to that given in the original work, although we note that the units of the limits are not the same as the units of the increment. Similar to Eq. (3), Eq. (1) can

* Corresponding author.
E-mail address: paul.stevenson@newcastle.edu.au (P. Stevenson).

0098-1354/$ – see front matter © 2009 Elsevier Ltd. All rights reserved.
doi:10.1016/j.compchemeng.2009.08.004

Nomenclature

A	surface interaction parameter ($\equiv 2\beta$)
c	concentration at the sub-surface ($\mathrm{mol\,m^{-3}}$)
c_b	bulk concentration ($\mathrm{mol\,m^{-3}}$)
D	coefficient of molecular dispersion ($\mathrm{m^2\,s^{-1}}$)
h	time increment (s)
k	a constant in the Freundlich isotherm ($\mathrm{mol^{(N-1)/N}\,m^{(3-2N)/N}}$)
K_F	a constant in the Frumkin isotherm ($\mathrm{m^3\,mol^{-1}}$)
K_H	Henry's law constant (m)
K_L	a constant in the Langmuir isotherm ($\mathrm{m^3\,mol^{-1}}$)
K_v	a constant in the Volmer isotherm ($\mathrm{m^3\,mol^{-1}}$)
m	an integer
M	number of time steps in a solution
n	an integer taking the value of between 1 and 2
N	consistency index in the Freundlich isotherm
r	radius of curvature of a spherical interface (m)
R	universal gas constant ($\mathrm{J\,K^{-1}\,mol^{-1}}$)
t	time (s)
T	absolute temperature (K)

Greek letters

γ	surface tension ($\mathrm{N\,m^{-1}}$)
γ_0	tension of a surfactant-free surface ($\mathrm{N\,m^{-1}}$)
Γ	surface excess ($\mathrm{mol\,m^{-2}}$)
Γ_∞	saturation surface excess ($\mathrm{mol\,m^{-2}}$)
Γ^*	equilibrium surface excess ($\mathrm{mol\,m^{-2}}$)
Π	surface pressure ($\mathrm{N\,m^{-1}}$)
τ	dummy variable with units of time (s)

be rewritten as

$$\Gamma(t) = \sqrt{\frac{D}{\pi}}\left\{2c_b\sqrt{t} - \int_0^t \frac{c(\tau)}{\sqrt{t-\tau}}\,d\tau\right\} \tag{4}$$

Thus it is seen that the first term in Eq. (3) is the same as the Ward–Tordai equation and the second term accounts for the influence of the curvature. As the radius of curvature tends to infinity the planar form of the Ward–Tordai equation is recovered.

Yang, Hung, Huang, and Lin (2008) comment that the trapezium rule is widely used for numerically integrating the back-diffusion term of the Ward–Tordai equation and many examples were given to support this statement. A detailed literature investigation showed, however, that only explicit schemes for a numerical solution to the Ward–Tordai equation were given by Miller and Kretzschmar (1980) and by the group of Nguyen (Phan, Nguyen, & Evans, 2005; Phan, Nguyen, & Evans, 2006), both of which lack a root-finding subroutine for the final term in the numerical integration and are therefore less accurate. On the other hand, many other investigations discussed by Yang et al. used various methods to directly solve the diffusion equations using various methods such as orthogonal collocation (Ziller & Miller, 1986) rather than the Ward–Tordai equation, and such methods are beyond the scope of the present study.

Phan et al. (2005, 2006) and Nguyen et al. (2006) proposed a numerical scheme for the planar Ward–Tordai equation and a similar scheme for the spherical (convex) version. Their methods were tested against experimental data for SDBS, Dowfroth D250 and β-casein. As will be shown later, their experimental data of SDBS seems to indicate that the rate of adsorption onto the inner surface of a droplet is faster than that onto the outer surface of a bubble, which defies common understanding of the physical processes in action.

We believe that we have developed a flexible and robust, yet efficient, numerical method of solving the Ward–Tordai equation that has utility for use in conjunction with a variety of adsorption isotherms, five of which are described in the following section. We do not claim to be the first to provide a numerical solution for the diffusion-controlled adsorption of non-ionic surfactants to the gas–liquid interface. We do, however, provide a simple solution to the Ward–Tordai equation that is easy to implement and robust, and we explicitly give pseudo-code to do so.

2. Relationship between surface excess and sub-surface concentration

The equation of Ward and Tordai was an important contribution to the theory of diffusion-controlled adsorption. However, it is not convenient to directly use the equation to explain experimental data since neither the surface excess nor the sub-surface concentration can be measured easily. Eastoe and Dalton (2000) gave five different equilibrium relationships to relate surface excess to sub-surface concentration (adsorption isotherms) which will be used in this work, and where possible the nomenclature of Eastoe and Dalton is retained. The source code provided in the supplementary material will adopt the following form for the adsorption isotherms:

1. *Henry's law isotherm*

$$\Gamma = K_H c \tag{5}$$

$$c = \frac{\Gamma}{K_H} \tag{6}$$

where K_H is the surface Henry's law constant. The corresponding surface equation of state is

$$\Pi = \gamma_0 - \gamma = nRT\Gamma \tag{7}$$

where Π is the surface pressure, γ is the surface tension and γ_0 is the surface tension of the liquid surface that is devoid of surfactant, n is an integer that takes the value of 1 for non-ionic surfactants and 2 for disassociated ionic surfactants, R is the universal gas constant and T is the absolute temperature. Note that the Ward–Tordai equation does not have utility for ionic surfactants, so n will take the value of unity throughout the present work.

2. *Langmuir isotherm*

$$\Gamma = \Gamma_\infty\left(\frac{K_L c}{1 + K_L c}\right) \tag{8}$$

$$c = \frac{1}{K_L}\frac{\Gamma}{\Gamma_\infty - \Gamma} \tag{9}$$

where K_L is a constant and Γ_∞ is the saturation surface excess. The corresponding surface equation of state is

$$\Pi = \gamma_0 - \gamma = -nRT\Gamma_\infty \ln\left(1 - \frac{\Gamma}{\Gamma_\infty}\right) \tag{10}$$

3. *Frumkin isotherm*

$$c = \frac{1}{K_F}\frac{\Gamma}{\Gamma_\infty - \Gamma}\exp\left[-A\left(\frac{\Gamma}{\Gamma_\infty}\right)\right] \tag{11}$$

where K_F is a constant and A is the surface interaction parameter. The corresponding surface equation of state is

$$\Pi = \gamma_0 - \gamma = -nRT\Gamma_\infty \ln\left(1 - \frac{\Gamma}{\Gamma_\infty}\right) - \frac{nRTA}{2}\Gamma_\infty\left(\frac{\Gamma}{\Gamma_\infty}\right)^2 \tag{12}$$

4. *Freundlich isotherm*

$$\Gamma = kc^{1/N} \tag{13}$$

$$c = \left(\frac{\Gamma}{k}\right)^{N} \tag{14}$$

where k is a constant and N is a consistency index. From this point, one can invoke Gibbs' isotherm, i.e.

$$\Gamma = -\frac{c}{nRT}\frac{d\gamma}{dc} \tag{15}$$

so that we can obtain the corresponding surface equation of state:

$$\Pi = \gamma_0 - \gamma = NnRT\Gamma \tag{16}$$

5. *Volmer isotherm*

$$c = K_v\left(\frac{\Gamma}{\Gamma_\infty - \Gamma}\right)\exp\left[\frac{\Gamma}{\Gamma_\infty - \Gamma}\right] \tag{17}$$

Again by invoking Gibbs' isotherm, we calculate the corresponding surface equation of state as

$$\Pi = \gamma_0 - \gamma = \frac{\Gamma_\infty^2}{\Gamma_\infty - \Gamma}nRT \tag{18}$$

3. Method of solution

To solve the Ward–Tordai equation numerically it is first written in the standard form of a Volterra equation of the second kind (Press, Teukolsky, Vetterling, & Flannery, 2007), i.e.

$$\Gamma(t) = g(t) + \int_0^t K(t, \tau, \Gamma(\tau))\,d\tau \tag{19}$$

where

$$g(t) = 2c_b\sqrt{\frac{D}{\pi}t} \tag{20}$$

$$K(t, \tau, \Gamma(\tau)) = -\sqrt{\frac{D}{\pi}}\frac{c(\Gamma(\tau))}{\sqrt{t-\tau}} \tag{21}$$

where $c(\Gamma(\tau))$ in Eq. (21) is a general adsorption isotherm. Note that Eq. (20) would give the evolution of surface excess if so-called 'back-diffusion' is neglected.

For a given step-size (i.e. time increment), h ($h>0$), if the solution at points $t_i = ih$, $i = 0, 1, \ldots, n-1$ is known then an approximation to $\Gamma(t_n)$ can then be computed by replacing the integral on the right side of Eq. (19) by a quadrature rule using values of the integrand at t_i, $i = 0, 1, \ldots, n$ and solving the resulting equation for $\Gamma(t_n)$. As $\Gamma(t_0) = g(0)$, the approximate solution can be computed in a stepwise manner. One of the simplest numerical integration methods is the trapezium rule; higher order methods require several simultaneous quadrature points in order to proceed with evolution of the solution. Poorly chosen starting values can give rise to unexpected instabilities in the integration. Adoption of the trapezium rule means that only one starting value of surface excess is required. Thus, using a simpler numerical integration method actually gives improved numerical performance compared to higher order quadrature methods. Employing the trapezoidal rule, and discretising Eq. (19) gives

$$\Gamma(t_n) = g(t_n) + h\left(\frac{1}{2}K(t_n, t_0, \Gamma(t_0)) + \sum_{j=1}^{n-1}K(t_n, t_j, \Gamma(t_j)) + \frac{1}{2}K(t_n, t_n, \Gamma(t_n))\right), \quad n = 1, 2, 3, \ldots \tag{22}$$

If $K(t, \tau, \Gamma(\tau))$ is linear, we can solve Eq. (22) directly for $\Gamma(t_n)$. In fact, if $K(t, \tau, \Gamma(\tau))$ is linear numerical methods are unnecessary as an analytical solution for the Ward–Tordai equation can be obtained (Sutherland, 1952). As most adsorption isotherms are non-linear, iterative techniques can be used to solve for $\Gamma(t_n)$ to within a desired accuracy range. Different iterative methods are available, and the choice depends mostly upon the complexity of the form of $K(t, \tau, \Gamma(\tau))$. For example, in the case of the Langmuir isotherm, the Newton–Raphson method, which requires the derivative of the $\Gamma(t)$, may be used as the derivative is readily computed. However, for more complex adsorption isotherms, the efficiency of the Newton–Raphson method may be compromised by the time required to evaluate the derivative. Moreover, if the derivative of $\Gamma(t)$ has singularities the method may not converge, making a more robust method highly desirable. The bisection method is such a robust iterative method (Press et al., 2007). In essence the bisection method continuously decreases the interval containing the root. It is seen from the nature of the method that the boundaries of the interval are critical to the efficiency. The interval used in the present solution is

$$\left(\Gamma(t_{n-1}),\ g(t_n) + h\left(\frac{1}{2}K(t_n, t_0, \Gamma(t_0)) + \sum_{j=1}^{n-1}K(t_n, t_j, \Gamma(t_j))\right)\right)$$

The robustness of the method is guaranteed by the fact that $\Gamma(t_{n-1})$ is always smaller than $\Gamma(t_n)$ (because surface excess rises monotonically) and that the upper boundary is only slightly larger than $\Gamma(t_n)$. It is noted that in the work of Phan et al. (2005, 2006) and Nguyen et al. (2006), this root-finding subroutine is absent, and $\Gamma(t_{n-1})$ was used to approximate $\Gamma(t_n)$. Since $\Gamma(t_{n-1})$ is smaller than $\Gamma(t_n)$, the effect of back-diffusion is therefore under-estimated. Because this under-estimation of back-diffusion occurs $n-1$ times, it is likely that the error may become significant at longer simulation times and may lead to a high sensitivity of the numerical accuracy to step-size and total step number.

The scheme described above can be readily adapted to solve the convex version of the Ward–Tordai equation (Eq. (2)) by making the modification:

$$g(t) = c_b\left(2\sqrt{\frac{D}{\pi}t} + \frac{D}{r}t\right) \tag{23}$$

and

$$K(t, \tau, \Gamma(\tau)) = -\sqrt{\frac{D}{\pi}}\frac{c(\Gamma(\tau))}{\sqrt{t-\tau}} - \frac{D}{r}c(\Gamma(\tau)) \tag{24}$$

4. Implementation of the scheme

Whilst numerical schemes for the solution of the Ward–Tordai equation are frequently mentioned in literature, we believe that no actual computer programs have ever been published. One reason for this phenomenon is that different researchers may prefer different computer languages; a piece of code written in one specific language may be of limited value to others. Therefore a pseudo-code of the above scheme is provided in Appendix A to make it possible to implement our scheme with any computer language. Furthermore, a flow chart is presented to aid the comprehension of the numerical scheme (Fig. 1) and the C++ source code is given in the supplementary material.

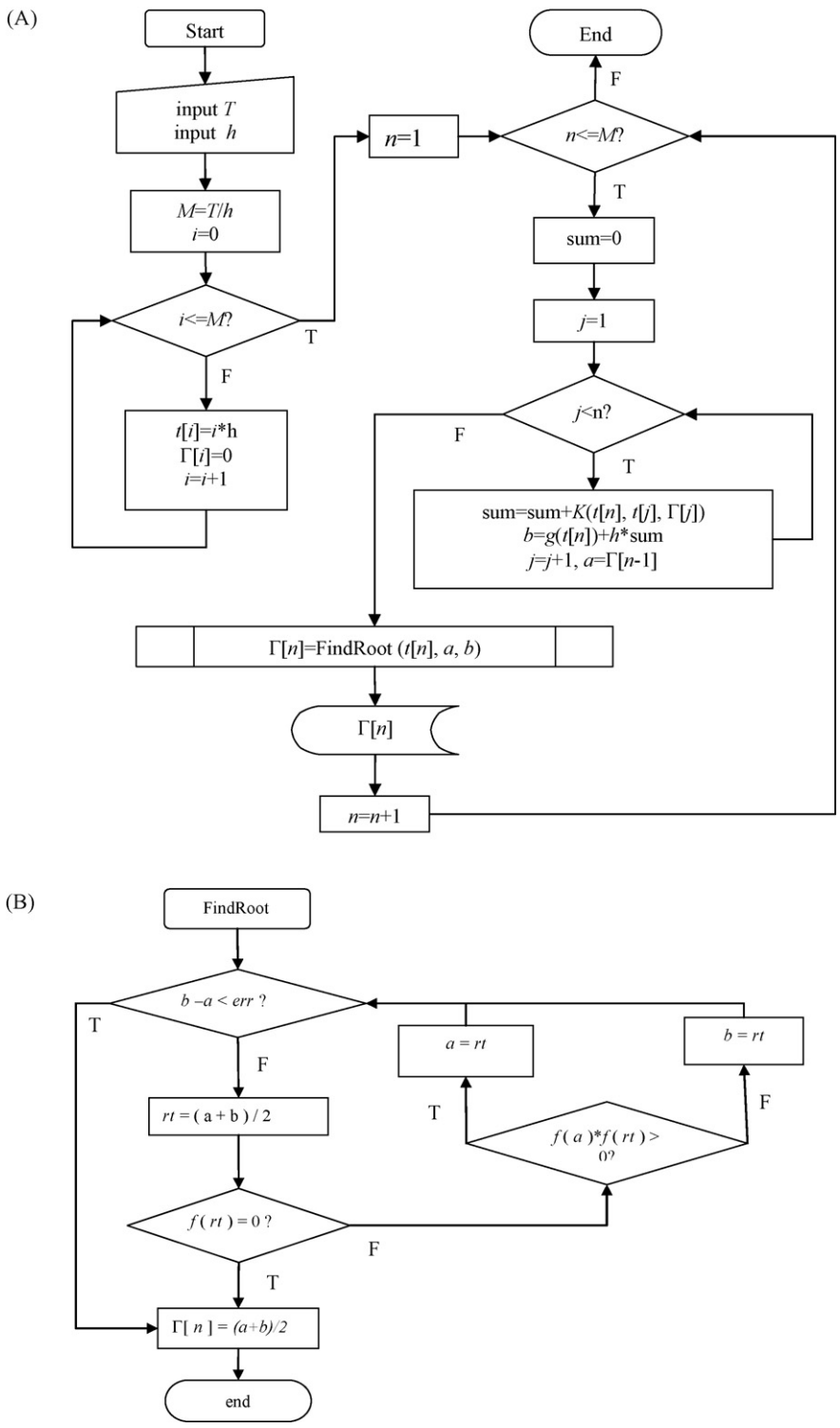

Fig. 1. Flowchart representation of the current numerical scheme. (A) The trapezium rule of integration, and (B) the bisection method of root-finding subroutine.

In order to further enhance the flexibility of the code, and for the sake of clarity, definitions of the functions g and K were not included in the pseudo-code. Since dimensional parameters are adopted in the current scheme, the expressions of g and K in most computer languages will be identical to Eqs. (20) and (21) for a planar interface, and Eqs. (23) and (24) for a convex interface, so the code is readily adapted to different isotherms and/or interfacial geometries. The singularity of Eq. (21) at $\tau = t$ was ameliorated in the present study by reducing the upper time limit by 0.01%.

5. Validation

When employing non-adaptive numerical integration there is a compromise between accuracy and efficiency when selecting the time increment. The numerical scheme described above

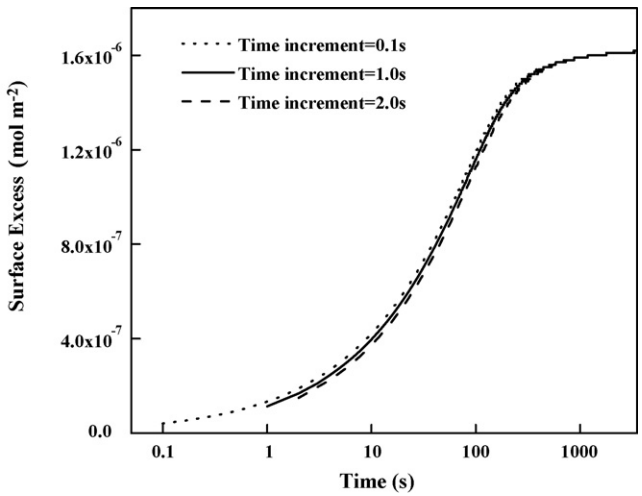

Fig. 2. Influence of step-size on the simulation result for the adsorption of $C_{10}E_8$ using the parameters of Yang and Gu (2004).

was implemented using C++ and the code was run at three different step-sizes: $h = 0.1$ s, 1.0 s, and 2.0 s for a total simulation time of 3000 s. The results are shown in Fig. 2. The Langmuir isotherm was used for simulation and values of model parameters include: $\Gamma_\infty = 1.8 \times 10^{-6}$ mol m^{-2}, $K_L = 1838$ m^3 mol^{-1}, $D = 5 \times 10^{-10}$ m^2 s^{-1}, $c_b = 5.44 \times 10^{-3}$ mol m^{-3}. These values are those given by Yang and Gu (2004) for the non-ionic surfactant $C_{10}E_8$. As the step-size decreases, the simulation result approaches the exact solution. However, the difference between the simulation results of the three different step-sizes is insignificant. It should be noted that our C++ code can typically complete the simulation within two seconds on a computer with a process frequency of 1.6 GHz when the step-size is 1 s and is therefore seen to be efficient.

Fig. 3 is a comparison between experimental data and the simulation results of the current scheme in conjunction with the Langmuir isotherm. Experimental data is for the non-ionic surfactant $C_{10}E_4$, as measured by Yang et al. (2008) using the pendant bubble method. Parameters used for simulation were: $D = 8.8 \times 10^{-10}$ m^2 s^{-1}, $\Gamma_\infty = 3.91 \times 10^{-6}$ mol m^{-2},

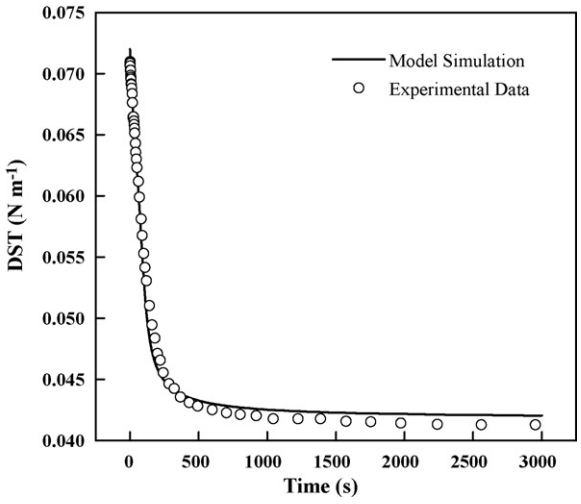

Fig. 3. A comparison between experimental dynamic surface tension (DST) data (Yang et al., 2008) and simulation results.

$K_L = 2146$ m^3 mol^{-1} and $r_b = 1.21 \times 10^{-3}$ m which were those obtained by Yang et al. (2008) by fitting experimental data to a finite element model. It is seen that the simulation results of the current model are in good agreement with Yang's experimental data, and thus in good agreement with their simulation results obtained by the finite element method. Consequently the efficacy of the current numerical method is proven.

6. The effect of interfacial geometry

The adsorption onto a planar interface or a convex interface can be treated as though the surfactant molecules are diffusing from an infinite external solution bulk, greatly simplifying the mathematical solution to the diffusion equations. It is due solely to this semi-infinite characteristic that Eqs. (1) and (2) have similar forms. In the case of the adsorption from inside a droplet to its inner surface (a closed finite system and a concave interface), the semi-infinite characteristic feature is absent thereby greatly increasing the complexity of the problem. Filippov and Filippova (1997) and Liggieri, Ravera, Ferrari, Passerone, and Miller (1997) studied the diffusion-controlled adsorption model for closed finite systems and Makievski et al. (1999) provided some experimental data on this topic. However, it was impossible to give an explicit expression similar to Eqs. (3) and (4). Miller, Fainerman, Aksenenko, Leser, and Michel (2004) did give an explicit expression as follows:

$$\Gamma = 2\sqrt{\frac{D}{\pi}}\left\{c_b\sqrt{t} - \int_0^t c(\tau)\, d\sqrt{t-\tau}\right\} \pm \frac{c_b}{r}Dt \tag{25}$$

and indicated that "the signs '−' or '+' before the second term on the right-hand side correspond to a drop or bubble, respectively". The authors did not give the derivation of this equation but cited the paper of Makievski et al. (1999), which only gave the short-time approximation of the adsorption onto a convex or concave interface; i.e.

$$\Gamma = 2c_b\sqrt{\frac{Dt}{\pi}} \pm \frac{c_b}{r}Dt \tag{26}$$

purposefully neglecting the effect of back-diffusion. It appears that Miller et al. (2004) simply combined the original Ward–Tordai equation (which accounts for both long- and short-time adsorption) with Eq. (26) to give Eq. (25). We believe that this procedure is erroneous and that Eq. (25) is incorrect except for in the short-time limit. Instead, for the adsorption onto a concave interface, implementation of the finite element method of Yang and Gu (2004) is suggested. Moreover, even if Eq. (25) is correct, Miller et al.'s statement makes sense only when the surfactant is contained in the heavy phase that forms the interface if the case of a liquid–liquid interface is considered. In the case that the surfactant is contained in the light phase, the direction of diffusion will be opposite and '+' will be for drop and '−' will be for bubble. As we are providing a general solution to the diffusion-controlled adsorption problem, it is necessary to use different nomenclature in order to avoid confusion. Therefore in the subsequent discussions, the term 'convex adsorption' will be used for the adsorption towards the outer surface of a sphere, and the term 'concave adsorption' will be used for the adsorption towards the inner surface of a sphere.

Makievski et al. (1999) observed the difference between the adsorption of a protein onto a convex surface and that onto a concave surface. Fig. 4 shows the simulation result of the current scheme compared with the result of a concave model of Yang and Gu (2004). The Langmuir adsorption isotherm was used and model parameters for $C_{10}E_8$ in pure water given were adopted. It

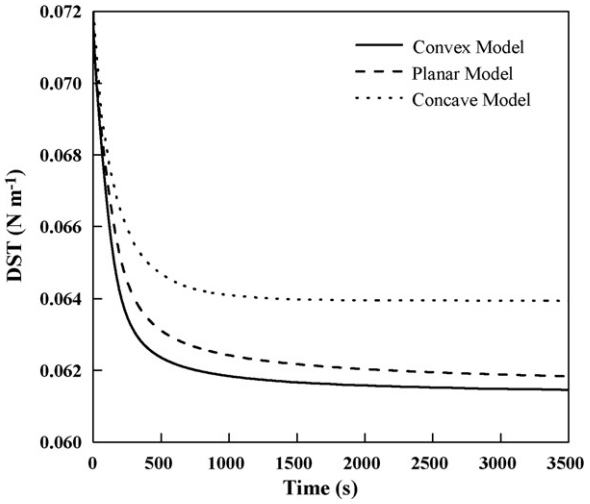

Fig. 4. Effect of interface geometry on the dynamic surface tension (DST) using the parameters of Yang and Gu (2004).

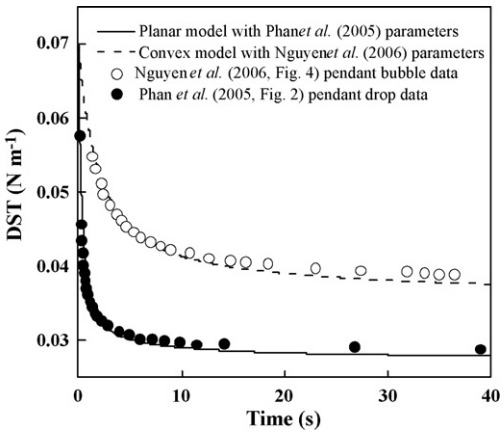

Fig. 5. A comparison between the convex adsorption data and concave adsorption dynamic surface tension (DST) data of the Nguyen group for 0.5 mM SDBS and the simulation results of the current numerical scheme. Parameters are listed in Table 1.

is seen that the relaxation of a planar surface or a convex surface is much faster than the concave surface. The reason is that both the convex model and the planar model can be treated as semi-infinite systems, whilst that of the concave model is a finite system. In a finite system, as molecules adsorb to the surface the concentration in the bulk of the liquid decreases due to mass conservation considerations. Therefore, equilibrium is not approached between the surface excess and the original bulk concentration, but rather an equilibrium between the surface excess and the depleted bulk concentration. In the cases of the convex and planar models, there is no such depletion of bulk concentration and we can infer that as the adsorption proceeds to long times, the surface excess of both cases will approach one another. However, the adsorption onto a convex surface is faster then that onto a planar surface. Adsorption onto a concave surface is slowest because of: (1) the geometry of the system, and (2) the fact that the bulk concentration becomes depleted.

Phan et al. (2005) reported data for the dynamic surface tension of a surface stabilised by 0.5 mM SDBS adsorbing to the gas–liquid interface using the pendant drop method (i.e. adsorbing to a concave interface), and the same researchers, Nguyen et al. (2006) reported data using the same solution using the pendant bubble method (i.e. a convex interface). The two data sets are shown in Fig. 5. The rate of adsorption onto the concave interface observed was faster than that onto a convex interface, whilst the equilibrium surface tension is lower. This result is contrary to the above theoretical analysis and to the observations of other authors, e.g. Makievski et al. (1999). In fact, the rate of adsorption to a convex interface is greater than the rate of adsorption to a concave interface, and the surface tension should approach a higher value in the pendant drop experiments because the bulk solution is depleted, whereas in the pendant bubble method it is not.

Despite the problems described with the data of the Nguyen group, we have run simulations using our numerical method using the two different sets of parameters reported by them and repeated here in Table 1. Our simulation results are in good agreement with the data of the Nguyen group by using $n = 2$ in Eq. (12) (i.e. that for a disassociated ionic surfactant). It is noted that in the work of Nguyen's group (Nguyen et al., 2006; Phan et al., 2005, 2006), the Ward–Tordai equation has been used to explain the adsorption of ionic surfactants (SDBS) and protein (β-casein) to interfaces; the Ward–Tordai equation is generally only valid for the adsorption of non-ionic surfactants (i.e. $n = 1$). The simulated values of surface excess are independent of n but the subsequent calculation of dynamic surface tension via the surface equation of state is dependent upon n. For guidance on the adsorption of ionic surfactants, please see the work of Vlahovska, Danov, Mehreteab, and Broze (1997). It should also be noted that the present simulation method generally completes in less than two seconds, whereas the VBA code of the Nguyen group takes several hours to run (Nguyen, 2008).

Measurement of dynamic surface tension using the pendant drop or pendant bubbles methods is based on the fact that the drop or bubble changes its shape as a result of interface relaxation. In general the bubble or droplet elongates. Wei, Yang, and Lin (2008) examined the influence of the deformation of the bubble in terms of bulk fluid motion; however its influence on the adsorption rate was not discussed. Yang et al. (2008) developed a finite element method for modelling the adsorption onto a convex surface which took into account the actual shape of the pendant bubble. The authors also measured the radius of curvature at the apex of the bubble during the measurement of dynamic surface tension and a 0.08 mm decrease was observed. As the finite element method takes into account the actual shape of the bubble, the method will become intractable if the changes in the shape of the bubble are considered. However, as a more flexible method, the current numerical scheme is able to incorporate changes in radius of curvature radius of curvature, simply by introducing a function giving the variation in radius of curvature.

Table 1
Adsorption parameters of 0.5 mol m^{-3} SDBS/water solution given by Phan et al. (2005) and Nguyen et al. (2006).

	T (K)	K_F (m^3 mol^{-1})	Γ_∞ (mol m^{-2})	A	D (m^2 s^{-1})	r (m)
Phan et al. (2005)	295	4.76	7.48×10^{-6}	0.032	4.76×10^{-10}	–
Nguyen et al. (2006)	295	7.95	4.83×10^{-6}	−0.114	1.97×10^{-11}	1.24×10^{-3}

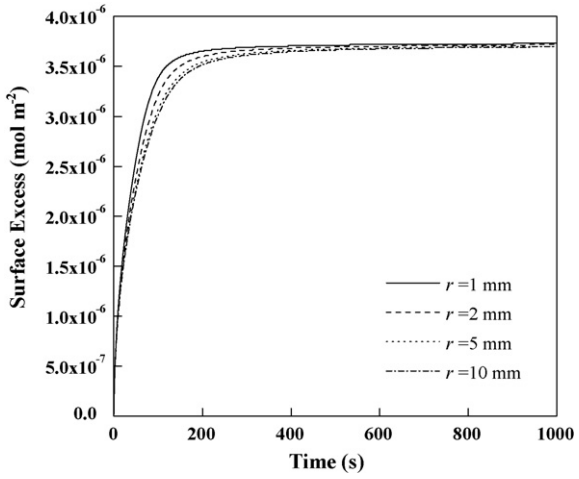

Fig. 6. Simulation results showing the effect of surface curvature on the adsorption rate. The legend indicates the radius of curvature of the bubble.

It is worthwhile investigating whether this added degree of complexity is necessary. Fig. 6 shows the simulation results of the adsorption onto convex surfaces of different radius of curvature, as listed in the legend. The other parameters are the same with that used in Fig. 2. It can be seen that, as expected, adsorption rate does depend on the radius of curvature. Adsorption rate decreases monotonically with increasing radius of curvature But as the change in the bubble/drop radius at apex during the measurement of dynamic surface tension is usually very small, its influence on the adsorption rate is negligible and provision for changes in curvature are generally unnecessary.

7. Conclusions

The equation of Ward and Tordai (1946) can be satisfactorily solved by the numerical method developed in the current work, which utilises the trapezium rule of numerical integration coupled with the bisection method of root-finding, thereby enhancing the robustness and accuracy of the method. The method also has utility for convex adsorption problems (i.e. for example the adsorption of non-ionic surfactants to the surface of bubbles), but not for concave adsorption problems (i.e. for example the adsorption of non-ionic surfactants to the surface of droplets). By applying the current numerical solution, the dependency of adsorption rate upon interface geometry has been examined. Simulation results showed that the adsorption to a convex interface in a semi-infinite system is much faster than the adsorption to a concave interface in a finite system, which is in agreement with the observation of Makievski et al. (1999). It is also found that the deformation of the bubble/drop during the dynamic surface tension measurement normally does not have significant impact on the adsorption rate.

Acknowledgments

We thank Dr. Stoyan Karakashev (Sofia University) and Prof. Anh Nguyen (University of Queensland) for useful discussions. This research was supported under the Australian Research Council's Discovery Projects funding scheme (project number DP0878979).

Appendix A. A pseudo-code

```
define f(x) = x-h/2*K (t, (1-10^-4)t, x )-b
read T, h
M = T / h
for i = 0 to M do,
   t [i] = i*h
  Γ[i ] = 0
endfor
for n = 1 to M do,
   sum = 0
   for j = 1 to n -1 do,
      sum = sum + K( t [ n ], t [ j ], Γ[ j ] )
   endfor
   b = g ( t [ n ] ) + h * sum
   a = Γ [ n - 1 ]
   j = 0
   repeat
      rt = ( a + b ) / 2
      if f( rt ) = 0 then do,
         Γ[ n ] = rt
         stop
      endif
      if f( a )*f( rt ) > 0 then do,
         a = rt
      else do,
         b = rt
      endif
      j = j + 1
   until b - a < err or j =M
   Γ[ n ] = rt
output Γ[n]
endfor
if j = M then do,
print, 'warning message:low accuracy'
```

Appendix B. Supplementary data

Supplementary data associated with this article can be found, in the online version, at doi:10.1016/j.compchemeng.2009.08.004.

References

Eastoe, J., & Dalton, J. S. (2000). Dynamic surface tension and adsorption mechanisms of surfactants at the air–water interface. *Advances in Colloid and Interface Science*, *85*, 103.

Filippov, L. K., & Filippova, N. L. (1997). Dynamic surface tension and adsorption kinetics in finite systems. *Journal of Colloid and Interface Science*, *187*, 352.

Liggieri, L., Ravera, F., Ferrari, M., Passerone, A., & Miller, R. (1997). Adsorption kinetics of alkylphosphine oxides at water/hexane interface. 2. Theory of the adsorption with transport across the interface in finite systems. *Journal of Colloid and Interface Science*, *186*, 46.

Lin, S. Y., McKeigue, K., & Maldarelli, C. (1990). Diffusion-controlled surfactant adsorption studied by pendant drop digitization. *AIChE Journal*, *36*, 1785.

Liu, J., Wang, C., & Messow, U. (2005). Adsorption kinetics at air/solution interface studied by maximum bubble pressure method. *Colloid and Polymer Science*, *283*, 139.

Makievski, A. V., Loglio, G., Krägel, J., Miller, R., Fainerman, V. B., & Neumann, A. W. (1999). Adsorption of protein layers at the water/air interface as studied by axisymmetric drop and bubble shape analysis. *Journal of Physical Chemistry B*, *103*, 9557.

Miller, R., Fainerman, V. B., Aksenenko, E. V., Leser, M. E., & Michel, M. (2004). Dynamic surface tension and adsorption kinetics of beta-casein at the solution/air interface. *Langmuir*, *20*, 771.

Miller, R., & Kretzschmar, G. (1980). Numerische lösung für ein gemischtes modell der diffusions-kinetik-kontrollierten adsorption. *Colloid and Polymer Science*, *258*, 85.

Mysels, K. J. (1982). Diffusion-controlled adsorption kinetics: General solution and some applications. *Journal of Physical Chemistry B*, *86*, 4648.

Nguyen, A. V. (2008). Personal communication.

Nguyen, A. V., Phan, C. M., & Evans, G. M. (2006). Effect of the bubble size on the dynamic adsorption of frothers and collectors in flotation. *International Journal of Mineral Processing*, *79*, 18.

Phan, C. M., Nguyen, A. V., & Evans, G. M. (2005). Dynamic adsorption of sodium dodecylbenzene sulphonate and Dowfroth 250 onto the air–water interface. *Mining Engineering*, *18*, 599.

Phan, C. M., Nguyen, A. V., & Evans, G. M. (2006). Dynamic adsorption of beta-casein at the gas–liquid interface. *Food Hydrocolloids*, *20*, 299.
Press, W. H., Teukolsky, S. A., Vetterling, W. T., & Flannery, B. P. (2007). *Numerical recipes: The art of scientific computing*. Cambridge: Cambridge University Press.
Sutherland, K. L. (1952). The kinetics of adsorption at liquid surfaces. *Australian Journal of Science Research Series A*, *5*, 683.
Vlahovska, P. M., Danov, K. D., Mehreteab, A., & Broze, G. (1997). Adsorption kinetics of ionic surfactants with detailed account for the electrostatic interactions. *Journal of Colloid and Interface Science*, *192*, 194.
Ward, A. F. H., & Tordai, L. (1946). Time-dependence of boundary tension of solutions. I. The role of diffusion in time-effects. *Journal of Chemical Physics*, *14*, 453.
Wei, H. H., Yang, M. W., & Lin, S. Y. (2008). An examination on the validity of the assumptions commonly made in dynamic surface tension measurement using a pendant bubble. *Colloids and Surfaces A*, *317*, 284.
Yang, C., & Gu, Y. (2004). Modeling of the adsorption kinetics of surfactants at the liquid–fluid interface of a pendant drop. *Langmuir*, *20*, 2503.
Yang, M. W., Hung, Y. L., Huang, H. F., & Lin, S. H. (2008). A study of $C_{12}E_4$ adsorption kinetics-considering pendant bubble shape. *Colloids and Surfaces A*, *317*, 462.
Ziller, M., & Miller, R. (1986). On the solution of diffusion controlled adsorption kinetics by means of orthogonal collocation. *Colloid and Polymer Science*, *264*, 611.